Study on mineral precipitation in fractured porous media using lattice Boltzmann methods

Mehrdad Ahkami[1,*], Andrea Parmigiani[2], Paolo R. Di Palma[3], Martin O. Saar[1], Xiang-Zhao Kong[1,+]

[1] Geothermal Energy and Geofluids, Institute of Geophysics, ETH Zurich, Sonneggstrasse 5, 8092 Zurich, Switzerland

[2] FlowKit Sàrl, Route dÓron2, 1000 Lausanne, Switzerland

[3]IRSA-CNR Water Research Institute, National Research Council, Via Salaria Km 29,300 C.P. 10 - 00015 Monterotondo Stazione, Rome, Italy

*mahkami@ethz.ch, +xkong@ethz.ch

Keywords: Lattice-Boltzmann method, Fractured porous media, Mineral precipitation.

ABSTRACT

Chemical, thermal and/or pressure equilibria of reservoirs are expected to be perturbed during various engineering/natural subsurface processes, such as geothermal energy extraction and geological CO_2 sequestration. Perturbation of subsurface equilibria often leads to chemical reactions, such as mineral dissolution/precipitation.

Unlike dissolution, precipitation of minerals can drastically influence the reservoir's permeability and the reservoir's ability to transmit mass and energy. The effect of precipitation on flow and transport in reservoirs depends on the extent and the pattern of the precipitated minerals in a porous medium. This implies that the deposition of precipitated minerals, occurring at the pore-scale, determines the continuum-scale changes in flow and transport properties. Therefore, a thorough understanding of the pore-scale deposition patterns of precipitated minerals is important for production optimization of subsurface reservoirs.

In the present work, we investigate pore-scale behaviour of single-species precipitation reactions in fractured porous media using a lattice Boltzmann method (LBM). Our LBM algorithm couples transport process and the single-species precipitation reactions. We simulate mineral precipitation, using a well-characterized fractured porous medium, consisting of one low-permeability and one high-permeability matrix. Each matrix is embedded with one flow-through and one dead-end fracture. We discuss the flow response (i.e., permeability variation) to precipitation reactions and the resulting mineral deposition patterns for various solute transport regimes and reaction rates. Our study provides insights into the coupling of the flow-reaction-geometry feedback loop in fractured porous media.

1. INTRODUCTION

Mineral precipitation is expected during various engineering/natural subsurface processes such as geothermal energy utilization (Wagner et al. 2005), hydrothermal alteration (Tenthorey 1998), and geological CO_2 sequestration (Kampman et al. 2014). The extent of mineral precipitation in the reservoirs depends on the pore-space geometry, transport regimes of species, and fluid-rock reaction rates. The regimes of species transport and fluid-rock reaction rates are generally quantified by two dimensionless numbers, the Damkohler number and the Peclet number. The Damkohler (Da) number is the ratio of the reaction rate to the transport rate, i.e.,

$$Da = \frac{k\delta}{D}, \qquad [1]$$

and the Peclet (Pe) number is the ratio of the advection rate of a substance to its diffusion rate,

$$Pe = \frac{u_d\delta}{D}, \qquad [2]$$

where k is the reaction rate, δ is the characteristic length, D is the diffusion coefficient, and u_d is the Darcy velocity.

Precipitation of minerals can drastically reduce the permeability of a porous medium and reorganize its flow field, which is due to pore-scale alterations, for example, of the flow path geometry, hydraulic connectivity, and surface roughness (Noiriel 2016). To investigate the evolution of mineral precipitation and its feedback on flow in porous media, different numerical simulation approaches, such as pore network models (Li et al. 2006), particle methods (e.g. Tartakovsky 2007, 2008), CFD based methods (Molins and Silin 2009, Yoon et al. 2012), and lattice Boltzmann methods (Parmigiani 2011), have been employed.

However, fractures are abundant in natural reservoirs, where fractures play a critical role in determining the flow and transport properties of reservoirs (Ebigbo et al. 2016). Fracture properties, such as opening, orientation, and connectivity, strongly influence the

interactions between fractures and the rock matrix, and subsequently the transport of mass and energy in reservoirs. The pore-scale alteration of these fracture properties, due to mineral precipitation, however, needs to be up-scaled in order to predict reservoir-scale permeability, and related fluid flow, changes.

In the presented study, we use the LBM approach, which has been successfully employed for pore-scale flow and transport simulations (e.g. Kang 2002, Walsh et al. 2009, Boek and Venturoli 2010), and follow the numerical approach of Huber et al. (2014) to simulate single-species precipitation reactions in a heterogeneous fractured porous medium that includes different rock matrices in which both flow-through and dead-end fractures have been embedded.

2. LATTICE BOLTZMANN METHOD

2.1 Fluid flow solver

In the framework of LBM, the fluid dynamics is explicitly solved based on kinetic theory, where the fluid flow is simulated via a discrete version of the Boltzmann equation. The macroscopic parameters, such as fluid pressure and velocity, are obtained through the measurement of the moments of the particle distribution function $f_i(x,v,t)$ (Huber et al. 2014). LBM often uses the bounce-back algorithm to handle solid boundaries, where f_i are reflected in the opposite direction, once they encounter a solid boundary. In LBM nomenclature, D_mQ_n is a commonly used term, where m defines the dimension of geometry, e.g. two- or three-dimensional, and n defines the number of streaming velocities. Here, we use the D_2Q_9 scheme (Figure 1). The LBM for fluid flow is described by the following discretized Boltzmann equation:

$$f_i(x, v_i\Delta t, t + \Delta t) = f_i(x,t) + \Phi_i(x,t) \qquad [3]$$

$$v_i = \begin{cases} (0,0) & i = 0 \\ (\pm 1,0), (0,\pm 1) & i = 1-4 \\ (\pm 1, \pm 1) & i = 5-8 \end{cases}, \qquad [4]$$

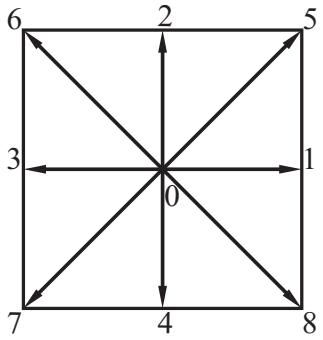

Figure 1: Lattice velocity indexing for D_2Q_9.

where x is the lattice position, i is one of the defined streaming velocities, t is time, Δt is the time step, v_i are the particle velocity vectors in lattice units, and $\Phi_i(x,t)$ is the collision operator that redistributes the particles by enforcing mass conservation, and is normally reduced to a single relaxation time (SRT or BGK) operator (Bhatnagar et al. 1954, Qian et al. 1992),

$$\Phi_i(x,t) = -\frac{1}{\tau}\left(f_i(x,t) - f_i^0(x,t)\right) \qquad [5]$$

$$\tau = \frac{\eta}{c_s^2} + \frac{1}{2} \qquad [6]$$

$$f_i^0(x,t) = w_i(x,t)\left[1 + \frac{u \cdot v_i}{c_s^2} + \frac{1}{2}\frac{(u \cdot v_i)^2}{c_s^4} - \frac{1}{2}\frac{u \cdot u}{c_s^2}\right] \qquad [7]$$

with τ being the relaxation time, η is the kinematic viscosity of the fluid, $c_s = 1/\sqrt{3}$ is the lattice sound velocity, f_i^0 is the local equilibrium distribution, w_i are the lattice weights for D_2Q_9 and u is the local macroscopic fluid velocity,

$$u(x,t) = \frac{1}{\sum_0^8 f_i(x,t)}\left[\sum_0^8 f_i(x,t)v_i\right] \qquad [8]$$

2.2 Transport solver for chemical reactants

The advection-diffusion equation for solute transport is then solved, employing a second set of lattices, i.e. $g_i(x,t)$, with a D_2Q_5 spatial discretization. With the Chapman-Enskog expansion (Succi 2001), our D_2Q_5 scheme yields the following advection-diffusion model

$$\frac{\partial C}{\partial t} + u \cdot \nabla C = \nabla \cdot (D \nabla C), \qquad [9]$$

where C is the species concentration and D is the species diffusion coefficient.

2.3 Heterogeneous mineral precipitation reaction

In the simulation of surface precipitation reactions, we deal with dynamic interface topologies (Kang et al. 2002, 2006). In this study, simulation of dynamic interfaces is done by solving the mass conservation equation at the fluid nodes, which are adjacent to the fluid-solid interfaces (Huber et al. 2014). The mass conservation equation in LBM system is given by

$$\Psi(\mathrm{x,t})_\mathrm{i} = w_i k C_0 \left(\frac{c}{C_0} - 1\right)^m, \qquad [10]$$

where k is the reaction rate, C_0 is the minimum concentration threshold for precipitation to occur, m is the order of reaction, and w_i is the lattice weights ($w_i = 1/3$ for $i=0$, and $w_i = 1/6$ in all other directions). We then define a continuous scalar variable, $\epsilon(x,t)$ at the reaction nodes, with a range from 0 (indicating a fluid node) to 1 (indicating solid node). As precipitation continues at a node, ϵ increases towards 1. The bounce-back algorithm is activated when $\epsilon(x,t) > 0.5$ at that node.

3. FRACTURED POROUS MEDIUM

In this study, we use a fractured porous medium with well-defined heterogeneities, including two porous matrices with two different pore sizes, each matrix containing one dead-end and one flow-through fracture. The complexity of this medium enables us to characterize precipitation patterns in a double-continuum medium. We previously used fluid flow visualization techniques to visualize fluid flow in an

identical, 3D-printed medium (Ahkami et al. 2018). The experimental investigation offers a statistical velocity validation for the LBM numerical results in such a medium.

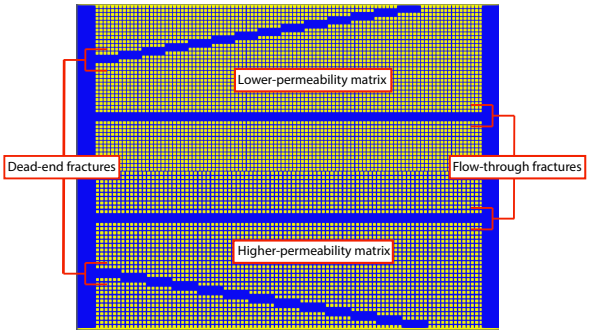

Figure 2: Fractured porous medium (blue: fluid nodes; yellow: solid nodes), consisting of low- and high-permeability matrices, flow-through fractures, and dead-end fractures.

In our numerical simulations, the dimension of the 2D medium is *2180* by *1680* nodes along the flow (longitudinal) and transverse (lateral) directions, respectively. The medium is equally divided into high- and low-permeability matrices with channel sizes of *6* and *4* nodes, respectively. Each matrix consists of square pillars with a dimension of 16×16 nodes. Moreover, each matrix contains one flow-through and one dead-end fracture. The fracture openings are *45* and *50* nodes wide for the fractures embedded in the low- and in the high-permeability matrices, respectively (Figure 2).

4. RESULTS AND DISCUSSION

We characterize the mineral precipitation patterns with the Da and the Pe numbers and list their ranges in Table 1, representing various solute transport and reaction rate regimes.

Table 1: Pe and Da numbers.

Pe	Da
10^{-3}	10^{-3}, 10^{-2}, 10^{-1}, 10^{0}, 2.5, 4
10^{-2}	10^{-3}, 10^{-2}, 10^{-1}, 10^{0}, 2.5, 4
10^{-1}	10^{-3}, 10^{-2}, 10^{-1}, 10^{0}, 2.5, 4
10^{0}	10^{-3}, 10^{-2}, 10^{-1}, 10^{0}, 4, 10, 20, 40
4	10^{-3}, 10^{-2}, 10^{-1}, 10^{0}, 4, 10, 40, 80,160

Lower Pe values indicate a diffusion-dominated regime, where the solute species are mainly transported by diffusion. Higher Pe numbers, on the other hand, indicate an advection-dominated solute species transport regime. For lower Da numbers, the reaction rate is lower than the transport rate of reactants and the system is reaction-limited. For higher Da numbers, the reaction rate is higher than the transport rate of the reactant and the system is transport-limited.

In our simulations, we first establish steady-state flow with a Darcy velocity of $u_d = 7.9 \times 10^{-5}$ $[l.u]$, without any reactions. Then a saturated fluid with $C = 1$ is injected from the inlet to trigger mineral precipitation. During the simulations, the precipitation threshold is set to $C_0 = 0.1$. We observe that mineral precipitation only takes place for some combinations of Pe and Da numbers. For these combinations, the simulations (and thus precipitation reactions) continue until the medium is clogged. Then the critical (end-time) porosity is calculated (Figure 3).

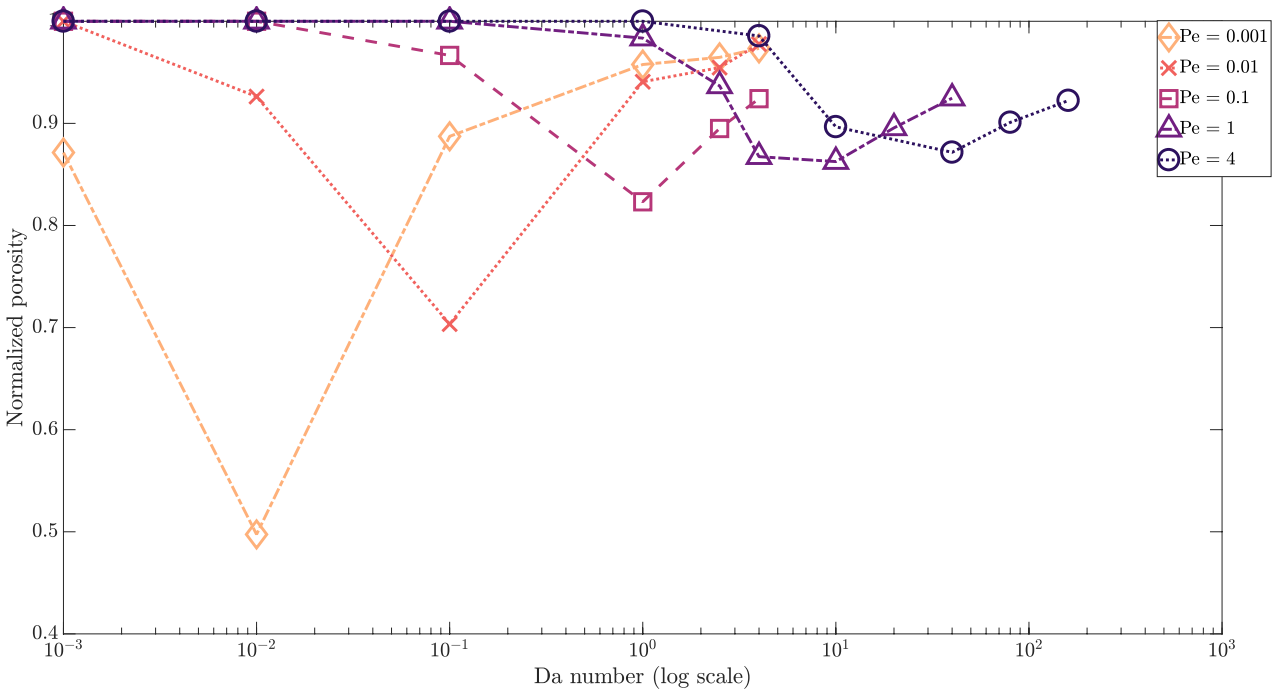

Figure 3: End-time porosity, normalized to the initial porosity, for different combinations of Pe and Da numbers.

The variation of end-time porosity values can be interpreted by different mineral precipitation scenarios. In the following, we discuss four specific precipitation regimes, observed in our fractured porous medium, namely a regime of no precipitation, a regime of inlet clogging, a regime of diffusive precipitation, and a regime of fracture isolation. Each of these regimes shows a different impact of mineral precipitation on the evolution of the permeability and other transport properties of reservoirs. In the following, we briefly discuss the observed impact of mineral precipitation on the permeability and fluid flow evolution in each of the scenarios.

4.1 Regime of no precipitation

Mineral precipitation, clogging the system, is not observed in the advection-dominated and reaction-limited regime (Table 2). In this regime, the reactants are mainly transported by advection through the higher-permeability features, i.e. fractures. In addition, the transport time is shorter than the reaction time, so that the reactants are transported to the next node before precipitation takes place. No reservoir damage due to mineral clogging is expected for geothermal systems with such a transport regime and reaction rate.

Table 2: Pe and Da numbers for the regime with no mineral precipitation.

Pe	Da
10^{-3}	-
10^{-2}	10^{-3}
10^{-1}	10^{-3}, 10^{-2}
10^{0}	10^{-3}, 10^{-2}, 10^{-1}
4	10^{-3}, 10^{-2}, 10^{-1}, 10^{0}

4.2 Regime of inlet clogging

Clogging of the inlet of a system is observed for systems that are diffusive and transport-limited (Table 3). Here, reactants are mainly transported by diffusion and the reaction time is shorter than the diffusion time. Such a mineral precipitation pattern is unfavourable for geothermal systems, as minerals precipitate close to the injection well, creating a zone of reduced permeability (Figure 4).

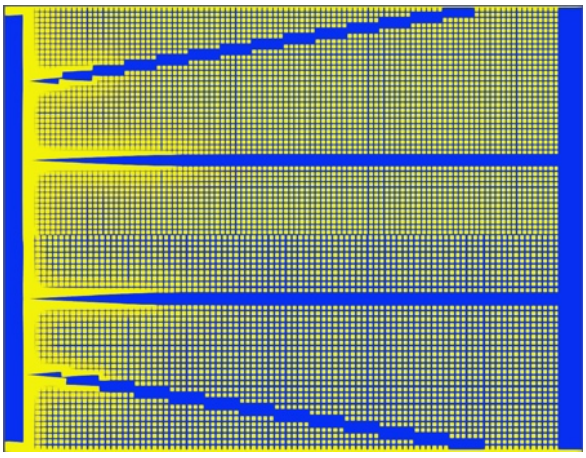

Figure 4: Regime of inlet clogging. The solid phase is shown in yellow and the pore space is shown in blue.

Table 3: Pe and Da numbers for the regime of inlet clogging.

Pe	Da
10^{-3}	10^{-1}, 10^{0}, 2.5, 4
10^{-2}	10^{0}, 2.5, 4
10^{-1}	-
10^{0}	-
4	-

4.3 Regime of diffusive precipitation

This type of mineral precipitation pattern is expected for a diffusive and reaction-limited regime (Table 4). The diffusive precipitation regime exhibits a longer reaction time, compared to the inlet clogging regime. Therefore, the reactants have enough time to spread into the matrices in the diffusive precipitation regime. Figure 5 shows a diffusive precipitation front. In a geothermal reservoir with such a precipitation regime, we expect a gradual decline of the overall system permeability and heat extraction efficiency with time.

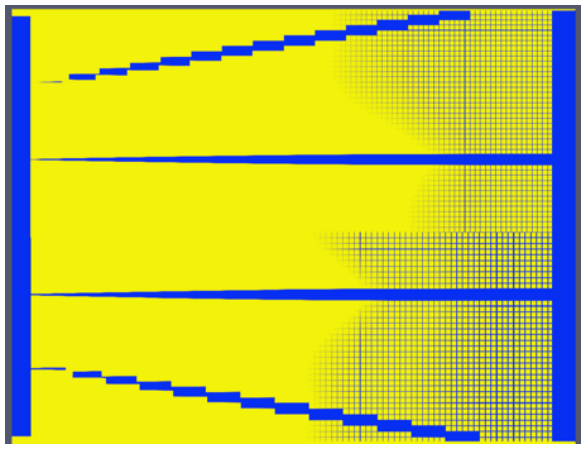

Figure 5: Diffusive precipitation regime. The solid phase is shown in yellow and the pore space is shown in blue.

Table 4: Pe and Da numbers for the regime of diffusive precipitation.

Pe	Da
10^{-3}	10^{-2}
10^{-2}	10^{-1}
10^{-1}	-
10^{0}	-
4	-

4.4 Regime of fracture isolation

In this regime, similar to the regime of no mineral precipitation, the reactants are mainly transported by advection, but the reaction rate is high enough for mineral precipitation to take place (Table 5). For such a configuration, mineral precipitation occurs mainly around the higher-permeability features (here fractures), which isolates the fractures from the surrounding matrices (Figure 6). If such mineral precipitation takes place in a geothermal system, the overall permeability of the system gradually decreases while the fractures remain open much longer. The

closure of the entire system requires a relatively long time. The heat extraction efficiency, on the other hand, decreases more significantly, because the surrounding rock matrices exhibit a large specific surface area and thus account for the majority of the heat energy extraction capacity.

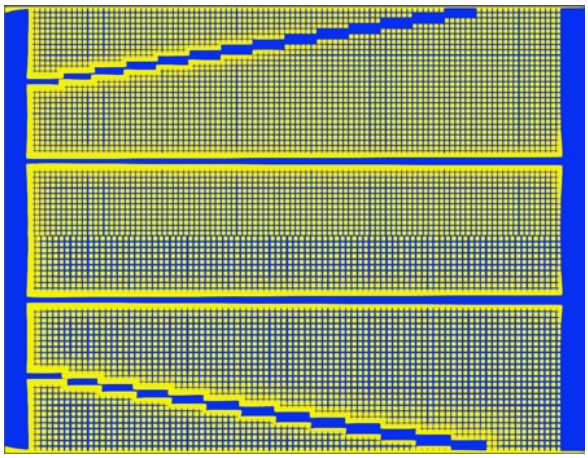

Figure 6: Fracture isolation regime. The solid phase is shown in yellow and the pore space is shown in blue

Table 5: Pe and Da numbers for the regime of diffusive precipitation.

Pe	Da
10^{-3}	-
10^{-2}	-
10^{-1}	10^{-1}
10^{0}	10^{0}, 4, 10, 20, 40
4	4, 10, 40, 80,160

5. CONCLUSIONS

In this study, we employ a lattice Boltzmann method (LBM) to study mineral precipitation in fractured porous media subjected to a wide range of Pe and Da numbers to evaluate from advective to diffusive and from reaction-limited to transport-limited systems. Based on our numerical results, we identify four different precipitation regimes: 1) a regime of no mineral precipitation, 2) a regime of inlet clogging, 3) a regime of diffusive mineral precipitation, and 4) a regime of fracture isolation. We also discuss the possible impact of the four observed reaction regimes on the lifetime of, and the efficiency of energy extraction from, geothermal systems.

Acknowledgements

This work was supported by ETH Grant ETH-12 15-2 and SNF Grant 177031. The Werner Siemens Foundation (Werner Siemens-Stiftung) is further thanked for its support of the Geothermal Energy and Geofluids Group at ETH Zurich.

REFERENCES

Ahkami, Mehrdad, Thomas Roesgen, Martin O. Saar, and Xiang-Zhao Kong. "High-resolution temporo-ensemble PIV to resolve pore-scale flow in 3D-printed fractured porous media." *Transport in Porous Media* (2018): 1-17.

Bhatnagar, Prabhu Lal, Eugene P. Gross, and Max Krook. "A model for collision processes in gases. I. Small amplitude processes in charged and neutral one-component systems." *Physical review* 94, no. 3 (1954): 511.

Boek, Edo S., and Maddalena Venturoli. "Lattice-Boltzmann studies of fluid flow in porous media with realistic rock geometries." *Computers & Mathematics with Applications* 59, no. 7 (2010): 2305-2314.

Ebigbo, Anozie, Philipp S. Lang, Adriana Paluszny, and Robert W. Zimmerman. "Inclusion-based effective medium models for the permeability of a 3D fractured rock mass." *Transport in Porous Media* 113, no. 1 (2016): 137-158.

Huber, Christian, Babak Shafei, and Andrea Parmigiani. "A new pore-scale model for linear and non-linear heterogeneous dissolution and precipitation." *Geochimica et Cosmochimica Acta* 124 (2014): 109-130.

Kampman, Niko, Mike Bickle, Max Wigley, and Benoit Dubacq. "Fluid flow and CO2–fluid–mineral interactions during CO2-storage in sedimentary basins." *Chemical Geology* 369 (2014): 22-50.

Kang, Qinjun, Dongxiao Zhang, Shiyi Chen, and Xiaoyi He. "Lattice Boltzmann simulation of chemical dissolution in porous media." *Physical Review E* 65, no. 3 (2002): 036318.

Kang, Qinjun, Peter C. Lichtner, and Dongxiao Zhang. "Lattice Boltzmann pore-scale model for multicomponent reactive transport in porous media." *Journal of Geophysical Research: Solid Earth* 111, no. B5 (2006).

Li, Li, Catherine A. Peters, and Michael A. Celia. "Upscaling geochemical reaction rates using pore-scale network modeling." *Advances in water resources* 29, no. 9 (2006): 1351-1370.

Molins, S., and D. Silin. "Pore-scale modeling of biogeochemical alteration of the transport properties of sediment." In *AGU Fall Meeting Abstracts*. 2009.

Noiriel, Catherine, Carl I. Steefel, Li Yang, and Dominique Bernard. "Effects of pore-scale precipitation on permeability and flow." *Advances in water resources* 95 (2016): 125-137.

Parmigiani, Andrea, C. Huber, Olivier Bachmann, and Bastien Chopard. "Pore-scale mass and reactant transport in multiphase porous media flows." *Journal of Fluid Mechanics*686 (2011): 40-76.

Qian, Y. H., Dominique d'Humières, and Pierre Lallemand. "Lattice BGK models for Navier-Stokes equation." *EPL (Europhysics Letters)* 17, no. 6 (1992): 479.

Tartakovsky, Alexandre M., Paul Meakin, Timothy D. Scheibe, and Rogene M. Eichler West. "Simulations of reactive transport and precipitation with smoothed particle hydrodynamics." *Journal*

of Computational Physics 222, no. 2 (2007): 654-672.

Tartakovsky, Alexandre M., G. Redden, Peter C. Lichtner, Timothy D. Scheibe, and Paul Meakin. "Mixing-induced precipitation: Experimental study and multiscale numerical analysis." *Water Resources Research* 44, no. 6 (2008).

Tenthorey, Eric, Christopher H. Scholz, Einat Aharonov, and Albert Léger. "Precipitation sealing and diagenesis: 1. Experimental results." *Journal of Geophysical Research: Solid Earth* 103, no. B10 (1998): 23951-23967.

Walsh, Stuart DC, Holly Burwinkle, and Martin O. Saar. "A new partial-bounceback lattice-Boltzmann method for fluid flow through heterogeneous media." *Computers & Geosciences* 35, no. 6 (2009): 1186-1193.

Wagner, Roland, M. Kühn, Volker Meyn, Hansgeorg Pape, Ullrich Vath, and Christoph Clauser. "Numerical simulation of pore space clogging in geothermal reservoirs by precipitation of anhydrite." *International Journal of Rock Mechanics and Mining Sciences* 42, no. 7-8 (2005): 1070-1081.

Yoon, Hongkyu, Albert J. Valocchi, Charles J. Werth, and Thomas Dewers. "Pore-scale simulation of mixing-induced calcium carbonate precipitation and dissolution in a microfluidic pore network." *Water Resources Research* 48, no. 2 (2012).